Available online at www.sciencedirect.com

SCIENCE DIRECT

Journal of Solid State Chemistry 178 (2005) 2167–2174

JOURNAL OF SOLID STATE CHEMISTRY

www.elsevier.com/locate/jssc

Rapid communication

Hydrothermal synthesis and luminescent properties of $BaBeF_4$: *RE* (*RE* = Eu, Tb)

Xiaotang Liu[a,b,*], Yalan Zhang[a], Chunshan Shi[c,*], Demin Xie[d]

[a] *Life Science and Chemistry School, Zhanjiang Normal College, Zhanjiang 524048, PR China*
[b] *College of Sciences, South China Agricultural University, Wushan Road, Tianhe District, Guangzhou 510642, PR China*
[c] *Key Laboratory of Rare Earth Chemistry and Physics, Changchun Institute of Applied Chemistry, Chinese Academy of Sciences, Changchun 130022, PR China*
[d] *Faculty of Chemistry, Northeast Normal University, Changchun 130024, PR China*

Received 17 December 2004; received in revised form 17 March 2005; accepted 19 March 2005
Available online 3 May 2005

Abstract

The $BaBeF_4$ powder has been hydrothermally synthesized from the double system. The effects of factors such as the ratio of initial reaction, pH value, reaction temperature and time were investigated. Moreover, the $BaBeF_4$: *RE* (*RE* = Eu, Tb) phosphors were prepared by the hydrothermal method. Further, they were characterized by means of X-ray powder diffraction, scanning electron microscopy, thermogravimetric analysis, infrared spectroscopy and X-ray photoelectron spectroscopy. The luminescent properties were investigated by the luminescence spectrometer. The results show that the molar ratio and pH in the initial reaction mixture associated with the reaction temperature dominate the crystallization of the products. The products are air stable. XPS confirms the oxygen content of those products is very low. $BaBeF_4$: *RE* obtained was pure phase of $BaBeF_4$. It indicates that doping a low concentration of RE^{3+} ions could not change the structure. In the co-doped Eu^{3+} and Tb^{3+} system, Eu^{3+}, Tb^{3+} and Eu^{2+} are observed in one matrix. These phenomena can be explained using an electron transfer theory. These *RE* ions occupy the sites of Ba^{2+} in $BaBeF_4$.

Keywords: Fluorides; Rare earth; Hydrothermal synthesis; Luminescent properties

---

1. Introduction

Complex fluorides, which show various interesting structures, have been extensively studied due to their particular physical properties, especially as photoluminescence host material [1,2]. Different isomorphous replacements in the framework of complex fluorides lead to many controllable properties [3]. It is well known that complex fluorides can be prepared by a conventional solid-state reaction. During the process, a calcinations step is required at high temperature for enhancing the diffusivity between raw solid materials. During calcinations, solid-state diffusion results in particle coarsening and agglomeration. And, this synthetic apparatus requires a complicated set-up because of the corrosive nature of fluoride. For improving the drawbacks of the solid-state reaction, various kinds of solution processes (or so called soft-chemical processes) have been investigated. Among the solution processing routes, the hydrothermal process has been proposed to be an effective method for synthesizing complex fluorides. In general, the hydrothermal process progresses in a closed system at a high autogenous pressure. By the benefit of the closed system with high pressure, the required temperature for preparing complex fluorides can be greatly reduced

---

*Corresponding authors. College of Sciences, South China Agricultural University, Wushan Road, Tianhe District, Guangzhou 510642, PR China. Fax: +86 208 528 2366.

E-mail addresses: jlxt33@126.com (X. Liu), cshi@ns.ciac.jl.cn (C. Shi).

0022-4596/$ - see front matter © 2005 Published by Elsevier Inc.
doi:10.1016/j.jssc.2005.03.032

because the reactivity of reactive species can be enhanced. Recently, mild hydrothermal and solvothermal synthesis of complex fluorides at 120–240 °C have been reported [4,5]. Herein we report a convenient method for the synthesis of $BaBeF_4$ and $BaBeF_4$: *RE* (*RE* = Eu, Tb) and examine the effects of the reaction temperature and time, solution pH value, ratio of initial composition on the products and investigate their luminescent properties.

2. Experimental

A series of complex fluorides $BaBeF_4$, which doped Eu or/and Tb were prepared by hydrothermal method, using BeF_2 (A.R.) and BaF_2 (A.R.)/$Ba(OH)_2$ (A.R.) as raw materials. The total mass of the starting materials was 1.5 g, precise ratio and reaction conditions are listed in Tables 1 and 2. A reaction mixture was obtained by mix BeF_2, BaF_2 or $Ba(OH)_2$, Eu_2O_3 (99.99%) or/and Tb_4O_7 (99.99%) in 9 mL deionized water, the NH_4HF_2 (A.R) was added dropwise to the mixture under magnetic stirring. The reaction mixture was transferred into a Teflon-lined autoclave of 20 mL capacity, and the autoclave was filled with water up to 75–80% of the total volume. Then hydrofluoric acid (40% mass, A.R.) was used to adjust the pH to 2–4. The autoclave was sealed into a stainless-steel tank and heated in an oven at 160, 200, 240 °C under autogenous pressure for 72, 96, 144 h. After cooling to room temperature, the resultant precipitate was centrifuged and washed with deionized water several times to pH ca. 7 and air-dried at room temperature. Excess ions were removed during washing.

Table 1
Hydrothermal synthesis conditions for $BaBeF_4$

Starting materials			*a*:*b*:*c* (mole ratio)	Reaction temperature/°C	Reaction time/h	pH	Phase in product
a	*b*	*c*					
$Ba(OH)_2$	BeF_2	NH_4HF_2	1:1:2	240	72	4	$BaBeF_4$
$Ba(OH)_2$	BeF_2	NH_4HF_2	1:2:2	240	72	4	$BaBeF_4$
$Ba(OH)_2$	BeF_2	NH_4HF_2	2:1:2	240	72	4	$BaBeF_4 + BaF_2$
$Ba(OH)_2$	BeF_2	NH_4HF_2	1:1:2	240	48	4	$BaBeF_4$
$Ba(OH)_2$	BeF_2	NH_4HF_2	1:1:2	200	72	4	$BaBeF_4$ + multiphase
$Ba(OH)_2$	BeF_2	NH_4HF_2	1:1:2	200	96	4	$BaBeF_4$
$Ba(OH)_2$	BeF_2	NH_4HF_2	1:1:2	160	72	4	$BaBeF_4$ + multiphase
$Ba(OH)_2$	BeF_2	NH_4HF_2	1:1:2	160	96	4	$BaBeF_4$
$Ba(OH)_2$	BeF_2	NH_4HF_2	1:1:2	240	72	2	$BaBeF_4$
$Ba(OH)_2$	BeF_2	NH_4HF_2	1:1:2	240	72	3	$BaBeF_4$
$Ba(OH)_2$	BeF_2	NH_4HF_2	1:1:2	240	72	6	$Be(OH)_2$ + multiphase
$Ba(OH)_2$	BeF_2	NH_4HF_2	1:1:2	240	72	8	$Be(OH)_2$
BaF_2	BeF_2	NH_4HF_2	1:1:0.5	240	72	4	$BaBeF_4$
BaF_2	BeF_2	NH_4HF_2	1:1:1	240	72	4	$BaBeF_4$
BaF_2	BeF_2	NH_4HF_2	1:2:1	240	72	4	$BaBeF_4$
BaF_2	BeF_2	NH_4HF_2	2:1:1	240	72	4	$BaBeF_4 + BaF_2$
BaF_2	BeF_2	NH_4HF_2	1:1:1	240	48	4	$BaBeF_4$ + multiphase
BaF_2	BeF_2	NH_4HF_2	1:1:1	200	72	4	$BaBeF_4$ + multiphase
BaF_2	BeF_2	NH_4HF_2	1:1:1	200	144	4	$BaBeF_4$
BaF_2	BeF_2	NH_4HF_2	1:1:1	160	144	4	$BaBeF_4$ + multiphase
BaF_2	BeF_2	NH_4HF_2	1:1:1	240	72	2	$BaBeF_4$
BaF_2	BeF_2	NH_4HF_2	1:1:1	240	72	3	$BaBeF_4$

Table 2
Hydrothermal synthesis condition of $BaBeF_4$: Eu, Tb

Starting materials					Mole ratio	Phase in product
$Ba(OH)_2$	BeF_2	NH_4HF_2	Eu_2O_3		0.98:1:2:0.02	$BaBeF_4$: Eu
$Ba(OH)_2$	BeF_2	NH_4HF_2		Tb_4O_7	0.98:1:2:0.02	$BaBeF_4$: Tb
$Ba(OH)_2$	BeF_2	NH_4HF_2	Eu_2O_3	Tb_4O_7	0.96:1:2:0.02:0.02	$BaBeF_4$: Eu, Tb
BaF_2	BeF_2	NH_4HF_2	Eu_2O_3		0.98:1:1:0.02	$BaBeF_4$: Eu
BaF_2	BeF_2	NH_4HF_2		Tb_4O_7	0.98:1:1:0.02	$BaBeF_4$: Tb
BaF_2	BeF_2	NH_4HF_2	Eu_2O_3	Tb_4O_7	0.96:1:1:0.02:0.02	$BaBeF_4$: Eu, Tb

All products were characterized by X-ray powder diffraction (XRD) on Rigaku D/max-II B diffractometer with a rotating target with Ni-filtered Cu-Kα radiation at room temperature. The XRD data for indexing and cell-parameter calculation were collected by a scanning mode with a step length of 0.02° in the 2θ range from 10° to 60° and a scanning rate of $0.2° \mathrm{min}^{-1}$. Silicon was used as an internal standard. Particle-size and morphology were observed on a Philips XL-30-EDAX scanning electron microscope (SEM). Powder samples were suspended in absolute ethanol by ultrasound for 10 min in an ultrasonic bath, then a few drops of the suspension were deposited onto a glass slice, dried, and sputter-coated with gold. Thermal gravimetric analysis (TGA) was performed using a Seiko instrument DG/DTA320 thermogravimetric system in air from ambient temperature to 800 °C at a heating rate of $5\,°\mathrm{C\,min}^{-1}$. Infrared (IR) spectra were obtained with a Nicolet 550-II spectrometer in the range 4000–400 cm^{-1}. The samples were pressed KBr pellets for the spectra measurements. X-ray photoelectron spectra (XPS) were recorded on a VG Scientific MAR-II X-ray photoelectron spectroscopy, using non-monochromated Mg Kα radiation as the excitation source. Binding energy values (Eb) were all referenced to carbon 1*s* line taken as 285.00 eV. Detecting vacuum is 1.33×10^{-1} Pa. Optical measurements were performed at room temperature using a Perkin Elmer LS 55 luminescence spectrometer.

3. Results and discussion

3.1. Synthesis

Table 1 lists the various reaction conditions for the synthesis of $BaBeF_4$. It seems that pure $BaBeF_4$ samples can be obtained by various reactants, which critical factors for obtaining the single-phase product are the ratio of initial composition, pH of the reaction system, reaction temperature and time. Fig. 1 shows SEM of some products. The effects of various conditions on the synthesis are described below.

3.1.1. Effect of the ratio of initial composition

The ratio of Ba/Be is a dominating factor for synthesis of $BaBeF_4$. When the Ba/Be ratio was 1 or 0.5, the powder formed was pure and of uniform grain, as shown in Fig. 1(a). However, when Ba/Be = 2, impurity phases appeared and the product formed was not uniform and even no clear grain formed existed, as shown in Fig. 1(b).

It is known that F^- ion is an effective mineralizer in both aqueous and non-aqueous systems [6,7]. In the synthesis of $BaBeF_4$, F^- ion was either a reactant or a mineralizer. Excess F^- ions may remarkably lower the temperature of crystallization. Thus $BaBeF_4$ can be crystallized even at 160 °C when excess F^- ions are added. Furthermore, when *RE* ions were doped in $BaBeF_4$, F^- ions play a role of charge compensation. And it can be found that addition of a small excess of

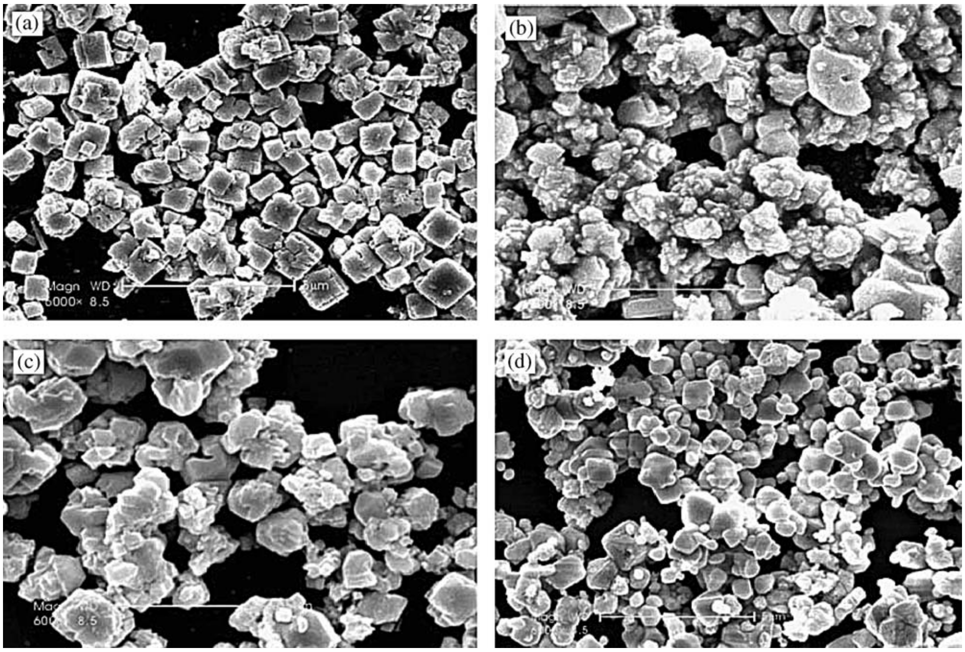

Fig. 1. (a) SEM for Ba/Be = 1 at 240 °C for 48 h, (b) SEM for Ba/Be = 2 at 240 °C for 72 h, (c) SEM for Ba/Be = 1 at 160 °C for 72 h, (d) SEM for Ba/Be = 1 at 200 °C for 72 h.

NH_4HF_2 did not result in the formation of impurities. In fact, NH_4HF_2 acts not only as a F^- source but also eliminates the risk of possible air pollution [8]. Therefore, some NH_4HF_2 was added to the reaction system, though the results show that the pure products can be prepared without NH_4HF_2 when BeF_2 and BaF_2 are used as raw materials.

3.1.2. *Effect of pH*

pH value is an important factor affecting the products. It can be found from Table 1 that single phase products were obtained using $Ba(OH)_2$ or BaF_2 as the barium source, as long as the pH is around 2–4. A high pH value often results in the presence of $Be(OH)_2$ or BaF_2. On the other hand, a pH value that is too low, e.g., $pH<2$, may cause HF gas pollution when the autoclave is opened. We note that NH_4HF_2 is a good system because it acts as the buffer agent to retain the pH during the reaction. So the suitable pH for the formation of the well-crystallized $BaBeF_4$ powder is around 4.

3.1.3. *Effect of reaction temperature and time*

To investigate the crystallization behavior of the precursor, the hydrothermal reaction was conducted at various temperatures for different times. In the $Ba(OH)_2$–BeF_2–NH_4HF_2–H_2O system, $BaBeF_4$ phase forms after the starting materials were heated at 160 °C for 72 h (Fig. 1(c)), but the grain is non-uniform. With increasing reaction time, the product crystallinity gradually increases. After reacting for 96 h, well-crystallized $BaBeF_4$ powders are obtained. And, at 200 °C for 72 h, $BaBeF_4$ phase also forms (Fig. 1(d)) but the grain is from non-uniform into uniform, after heating for 96 h, the pure $BaBeF_4$ products are obtained. Single phase $BaBeF_4$ can be prepared after the mixture heated at 240 °C for 48 h (Fig. 1(a)). It is obvious that $BaBeF_4$ can be crystallized below 240 °C, but prolonged reaction time is required because the transformation from oxide to fluoride is a slow process at low temperature in hydrothermal condition. In the BaF_2–BeF_2–NH_4HF_2–H_2O system, the pure phase $BaBeF_4$ cannot be obtained at 160 °C for 144 h or at 200 °C for 72 h. Although the $BaBeF_4$ phase begins to form at 160 °C, a temperature higher than 200 °C is necessary for preparation of the well-crystallized powder because the crystallinity increases with increasing temperature. Thus, the borderline conditions for the hydrothermal preparation of the $BaBeF_4$ are (l)a temperature higher than 200 °C and (2)a time longer than 48 h.

3.1.4. *Synthesis of $BaBeF_4$: RE (RE = Eu, Tb)*

$BaBeF_4$: *RE* (*RE* = Eu, Tb) were prepared by hydrothermal synthesis when pH = 4, $T = 240$ °C, $t = 72$ h, 0.02 mole ratio *RE* ions doped. The conditions were given as Table 2.

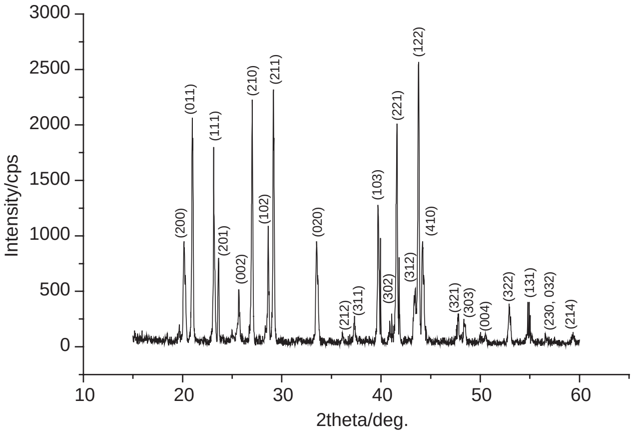

Fig. 2. The XRD patterns of $BaBeF_4$: 0.02Eu, 0.02Tb.

Table 3
The XRD data of $BaBeF_4$: 0.02 Eu, 0.02Tb

Peak No.	Experimental data		JCPDS Card 20-118 data		
	d value	I/I_1	*d* value	I/I_1	*hkl*
1	4.4052	37	4.40	35	200
2	4.2297	80	4.23	75	011
3	3.8427	70	3.83	70	111
4	3.7588	31	3.74	30	201
5	3.5188	20	3.520	16	002
6	3.2972	86	3.380	65	210
7	3.1150	42	3.270	60	102
8	3.0600	90	3.060	80	211
9	2.6725	36	2.652	35	020
10	2.4873	5	2.442	4	212
11	2.4075	11	2.430	10	311
12	2.2692	49	2.270	40	103
13	2.2551	38	2.259	35	302
14	2.1693	78	2.168	55	221
15	2.0769	18	2.080	20	312
16	2.0645	100	2.065	100	122
17	2.0483	37	2.040	35	410
18	1.9000	11	1.892	6	321
19	1.8722	10	1.834	18	303
20	1.7885	5	1.758	6	004
21	1.7287	15	1.719	10	322
22	1.6738	16	1.687	12	131
23	1.6252	5	1.650	12	230
			1.595	10	032
24	1.5556	5	1.561	6	214

3.2. *Characterization of $BaBeF_4$: 0.02Eu, 0.02Tb*

The XRD patterns of all products were characterized. Fig. 2 shows the XRD patterns of $BaBeF_4$:0.02Eu, 0.02Tb. No other peaks or impurities are detected. Therefore, XRD confirmed the phase purity of the resulting $BaBeF_4$ obtained from hydrothermal method. The compound crystallizes in the orthorhombic; the indexed powder XRD patterns are listed in Table 3. The lattice parameters were optimized by least-square refinements. The unit cell parameters for the product are $a = 8.8104$, $b = 5.3450$, $c = 7.0376$, which is in good agreement with those given in [JCPDS Card 20-118].

The result shows that at the dopant concentration of $0.02\,\mathrm{mol\,mol^{-1}}$ Eu^{3+} and $0.02\,\mathrm{mol\,mol^{-1}}$ Tb^{3+} the obtained product was pure phase of $BaBeF_4$, or the product is free from impurities. It indicated that the product was single phase and the structure could not be changed by a low doping concentration of *RE* ions.

The values of the unit cell parameters are slightly higher than those for the corresponding phase $BaBeF_4$ prepared by solid-state reaction. Under mild hydrothermal synthesis, the reactant ions can move freely in the solution and make contact with each other slowly and directionally. This type of reaction makes the direction more symmetrical than that of a solid state reaction. As a result, the lattice parameter of the product synthesized by the hydrothermal method is larger than that synthesized by the solid-state method.

The morphology of the samples were examined by SEM at room temperature. Fig. 3 shows the scan electron micrograph of $BaBeF_4$: 0.02Eu, 0.02Tb. As can be seen from this figure, the powder is homogeneous with good shape, indicating that the product is a pure phase. Uniform grain texture of $BaBeF_4$ can be observed with grain sizes ranging from 600 to 700 nm.

The thermal stability of the $BaBeF_4$: 0.02Eu, 0.02Tb were studied by TG-DTA analyses in air, as shown in Fig. 4. There are no phase transformations up to 800 °C and a small mass of ca. 1.2% surface water was evident. IR of $BaBeF_4$: 0.02Eu, 0.02Tb (Fig. 5) confirms the presence of water. The observation of a sharp absorption band around $3420\,\mathrm{cm^{-1}}$ indicates the presence of terminal hydroxyl groups. The $1637\,\mathrm{cm^{-1}}$ band is due to the H–O–H bending vibrations of the H_2O molecule, which is indicative of the presence of water in the sample. The results show that the sample is stable in air and the surface water is removed upon increasing the temperature.

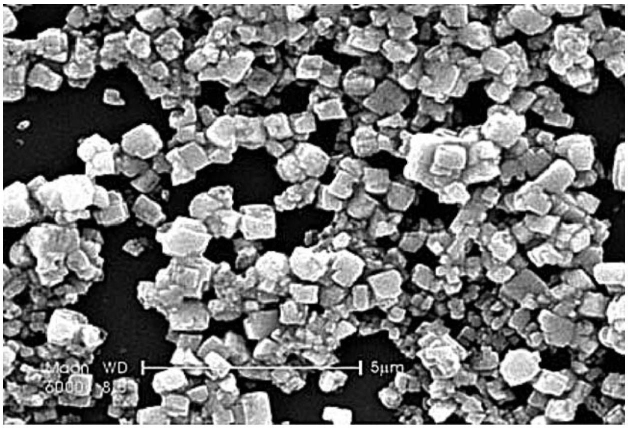

Fig. 3. SEM of $BaBeF_4$: 0.02Eu, 0.02Tb.

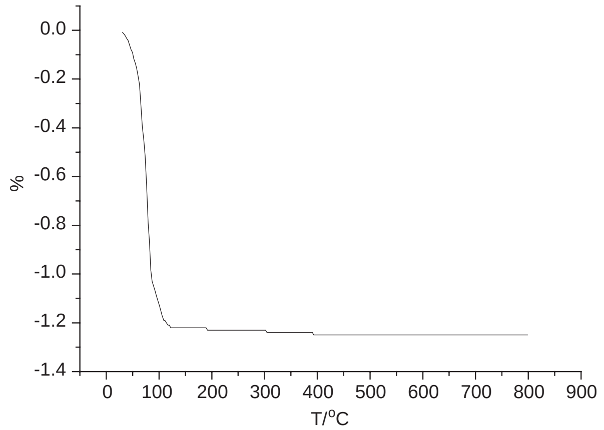

Fig. 4. TG of $BaBeF_4$: 0.02Eu, 0.02Tb.

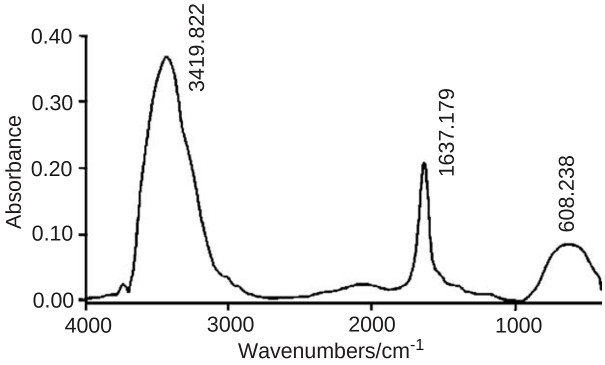

Fig. 5. IR of $BaBeF_4$: 0.02Eu, 0.02Tb.

3.3. Luminescent properties

To study the luminescent properties of $BaBeF_4$: *RE* (*RE* = Eu, Tb), we measure their excitation and emission spectra after they are dried at 80 °C for 2 h to remove the surface water.

3.3.1. Luminescence of $BaBeF_4$: Eu

Fig. 6 shows the excitation spectrum of $BaBeF_4$: Eu phosphor. The excitation spectrum has a number of line peaks belonging to the f–f transition of Eu^{3+} due to the transitions between the ground state ($^7F_0$) of Eu^{3+} and its excitation state (^5D_J) ($J = 0, 1, 2, 3$). It is well known that the broadband at about 280 nm is attributed to the charge transfer band (*CTS*) between Eu^{3+} and the rounding O^{2-} ions. This result shows that the oxygen content of those products is much lower than that of $BaBeF_4$ synthesized by solid-state reaction. In fact, there is hardly any insertion of oxygen. In addition to the excitation spectrum, we have obtained strong evidence of the formation of $BaBeF_4$: Eu from the XPS.

It is well known that the oxygen content of those complex fluorides, which were prepared by solid-state reaction at high temperature, is very high although the

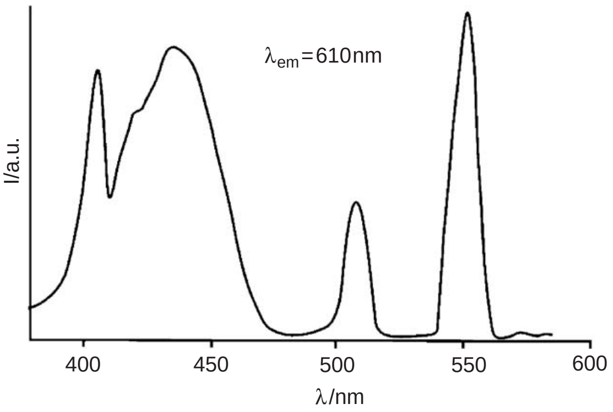

Fig. 6. Excitations spectrum of $BaBeF_4$: Eu.

reactions were processed under inert gas protection. In the hydrothermal synthesis system, OH^- is present. Because the OH^- ionic radius is similar to that of F^- ion, complex fluorides containing oxygen may be obtained. How about the oxygen content of the samples? XPS may be an effective method for detecting oxygen content. XPS data provide information on the chemical state of the elements in the near-surface region. If the samples prepared by hydrothermal method contained oxygen, the electron binding energy (Eb) of the atom inner shell would change with the change of the chemical environment, thus the Eb would change too. The F(l*s*), Ba($3d_{5/2}$) and Be(l*s*) XPS of $BaBeF_4$: 0.02Eu synthesized by hydrothermal method are shown in Fig. 7(a)–(c). It can be seen from Fig. 7(a) that the F(l*s*) binding energy is 685.3 eV, and the symmetrization of the peak shape is very good. Furthermore, the peak shape is in correspondence with that of BaF_2 as reference. The result indicates that O–F bond has not been formed in $BaBeF_4$: 0.02Eu. No distinct difference between Ba($3d_{5/2}$), Be(l*s*) of $BaBeF_4$: 0.02Eu and the references BaF_2, BeF_2 is observed. Therefore, the typical Be–F and Ba–F had been present for both obtained and standard. The result shows that the content oxygen of $BaBeF_4$: 0.02Eu synthesized by hydrothermal method is very low. The binding energy of the elements in $BaBeF_4$: 0.02Eu were listed in Table 4.

Fig. 8 shows the emission spectrum of Eu^{3+}-doped $BaBeF_4$ under 320 nm excitation. The main features are the ${}^5D_0$–${}^7F_J$ $(J = 0, 1, 2, 3, 4)$ transition of Eu^{3+} are observed and are marked in the figure. The intense peak in the spectrum is ~595 nm, corresponding to the ${}^5D_0$–${}^7F_1$ transition as is the case with Eu^{3+}-doped samples.

It is well known, as is to be expected, that the spectral energy distribution of the emission from the ${}^5D_0$ level depends strongly on the crystal structure. As long as the Eu^{3+} ions occupy one crystallographic site in the host lattice only sharp emission lines are expected; not more than three for the ${}^5D_0$–${}^7F_1$, not more than five for the ${}^5D_0$–${}^7F_2$ transition in view of the degeneracy of the level involved. If more than one crystallographic site is occupied, these numbers can be higher due to the presence of different types of Eu^{3+} centers. If the Eu^{3+}

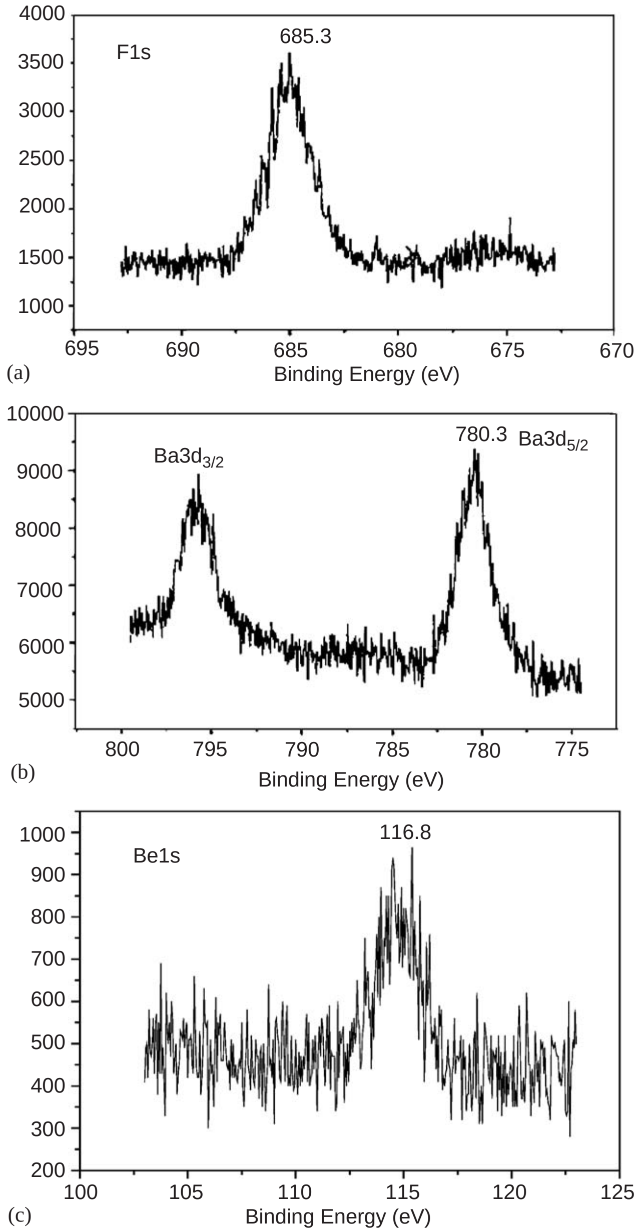

Fig. 7. XPS of $BaBeF_4$: Eu.

Table 4
The binding energy of the elements in $BaBeF_4$: 0.02Eu (eV)

Compounds	F_{1s}	Be_{1s}	$Ba_{3d_{5/2}}$
$BaBeF_4$	685.3	116.8	780.3
BeF_2	685.8	116.9	
BaF_2	685.4		780.6

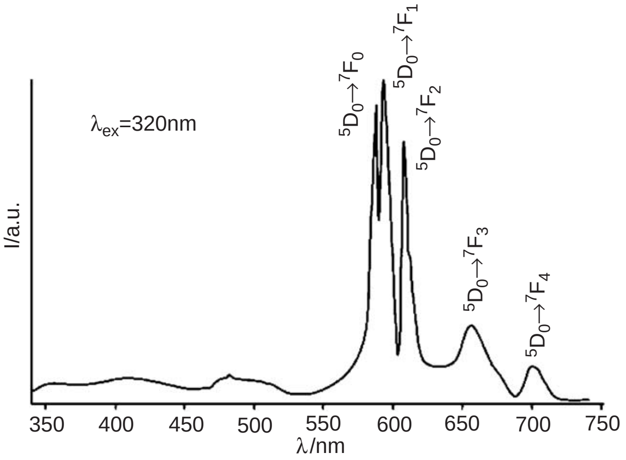

Fig. 8. Emission spectrum of $BaBeF_4$: Eu.

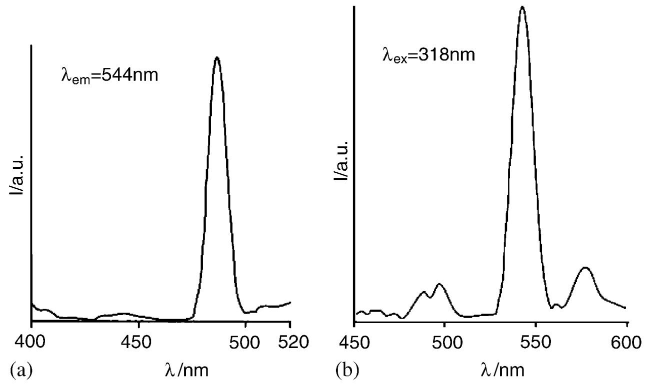

Fig. 9. Excitation (a) and emission (b) spectra of $BaBeF_4$ Tb.

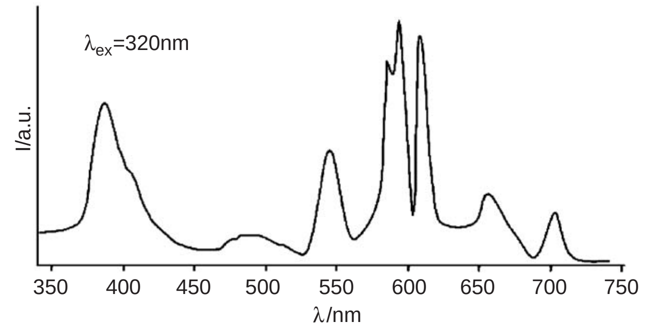

Fig. 10. Emission spectrum of $BaBeF_4$: Eu, Tb.

ions would occupy the position with inversion symmetry, the $^5D_0$–$^7F_1$ emission lines are expected to have the highest intensity in view of their magnetic dipole character [9]. If the Eu^{3+} ions would occupy the position which is no inversion symmetry (C_s symmetry), the $^5D_0$–$^7F_2$ emission is expected to be dominant [10]. In these case, the $^5D_0$–$^7F_1$ transitions have the highest intensity, demonstrating that the Eu^{3+} ions occupy centrosymmetrical site in $BaBeF_4$. XRD and crystal structure show that Ba^{2+} ions are located in the center of symmetry. And the ionic radius of Eu^{3+} is more similar to that of Ba^{2+} than that of Be^{2+}. So we conclude that Eu^{3+} ions occupy one crystallographic site in the $BaBeF_4$, which are the Ba^{2+} sites.

Although Eu^{3+} can be reduced to Eu^{2+} ions, there is hardly any emission of Eu^{2+} in the emission spectrum of $BaBeF_4$: Eu. The phenomenon can be explained as follows: the stable valance of Eu is a trivalent charge state (Eu^{3+}), on the other hand, the reaction temperature of hydrothermal synthesis is lower and the conditions are mild, so the valance change is not easy. Besides these, there are a plenty of F^- ions in the system, which act as charge compensation in the $BaBeF_4$ and make Eu^{3+} be stable in the matrix.

3.3.2. Luminescence of $BaBeF_4$: Tb

The excitation spectrum of Tb^{3+} ion is attributed to $4f$–$4f$ transitions, as shown in Fig. 9(a). The emission peaks of Tb^{3+} are attributed to $^5D_3$–^7F_J and $^5D_4$–^7F_J transitions, and the strongest peak is at 544 nm, as Fig. 9(b).

3.3.3. Luminescence of $BaBeF_4$: Eu, Tb

The emission spectrum of $BaBeF_4$: Eu, Tb phosphor is given in Fig. 10.

Eu^{3+}, Tb^{3+} and Eu^{2+} can coexist in one system. The group of sharp peaks ranging 560~720 nm is the emission of Eu^{3+}, which due to the $^5D_0$–^7F_J ($J = 0, 1, 2, 3, 4$) transition. The emission line at 544 nm, is a characteristic emission from $^5D_4$–$^7F_5$ transition of Tb^{3+} ion. The Eu^{2+} ions exhibit broadband fluorescence, which corresponds to $5d$–$4f$ transitions in Eu^{2+}. The strongest emission peak is found at 388 nm with a shoulder peak at 402 nm. The Eu^{2+} ions occupy the Ba^{2+} sites of $BaBeF_4$, which are surrounded by eight fluorine ions.

Eu^{3+} and Tb^{3+} is a couple of conjugate rare earth ions, thus, an electron transfer can take place between Eu^{3+} and Tb^{3+} ions [11]:

$$Eu^{3+}(4f^6) + Tb^{3+}(4f^8) = Eu^{2+}(4f^7) + Tb^{4+}(4f^7).$$

When Eu^{3+} and Tb^{3+} are codoped in a $BaBeF_4$ matrix, an electron can be transferred from a $Tb^{3+}(4f^8)$ to an $Eu^{3+}(4f^6)$ to get their half-filled $4f$ shell configuration ($4f^7$). This explanation can be identical with the relative emission intensity. Under the same excitation conditions, the emission intensity of Eu^{3+} and Tb^{3+} is decreased whereas that of Eu^{2+} is increased.

4. Conclusion

$BaBeF_4$ can be synthesized by mild hydrothermal method. The results show that the molar ratio and pH in the initial reaction mixture associated with the reaction temperature dominate the crystallization of the products. The products are air stable. XPS confirms the oxygen content of those products is very low. $BaBeF_4$: *RE* obtained was pure phase of $BaBeF_4$.

It indicates that doping a low concentration of RE^{3+} ions could not change the structure. In the codoped Eu^{3+} and Tb^{3+} system, Eu^{3+}, Tb^{3+} and Eu^{2+} are observed in one matrix. These phenomena can be explained using an electron transfer theory. These *RE* ions occupy the sites of Ba^{2+} in $BaBeF_4$.

Acknowledgments

This work was supported by National Nature Science Foundation of China (90201032).

References

[1] A. Meijerink, J. Lumin. 55 (1993) 125.
[2] Y. Tan, C. Shi, J. Solid State Chem. 150 (2000) 178.
[3] K. Somaiah, M.V. Narayana, Mater. Chem. Phys. 24 (1990) 353.
[4] C. Zhao, S. Feng, R. Xu, C. Shi, J. Ni, Chem. Commun. (1997) 945.
[5] R. Hua, Z. Jia, D. Xie, C. Shi, Mater. Res. Bull. 37 (2002) 1189.
[6] C. Zhao, S. Feng, Z. Chao, C. Shi, R. Xu, J. Ni, Chem. Commun. (1996) 1641.
[7] M. Estermann, L.B. Mccusker, C. Baerlocher, A. Merrouche, H. Kessler, Nature 352 (1991) 320.
[8] X. Xun, S. Feng, R. Xu, Mater. Res. Bull. 33 (1998) 369.
[9] G. Blasse, A. Bril, W.C. Nieuwpoort, J. Phys. Chem. Solids 27 (1966) 1587.
[10] G. Blasse, A. Bril, J. Inorg. Nucl. Chem. 27 (1967) 2231.
[11] Shi Chun-Shan, Su Qiang. The Chemistry and Physics of Abnormal Valency Rare Earth Elements, Science Press, Beijing, 1994, pp. 28–41 (in Chinese).